BMC Plant Biology

RESEARCH

Open Access

Effect of nanocellulose-assisted green-synthesized iron nanoparticles and conventional sources of Fe on pot marigold plants symbiotically with arbuscular mycorrhizal fungus (*Funneliformis mosseae*)

Maryam Nohesara[1], Elham Malekzadeh[1*], Mojtaba Barani Motlagh[1] and Aliasghar Tatari[2]

Abstract

The objective of this study was to investigate the effect of nanocellulose-assisted green-synthesized iron nanoparticles (FeNPs) and conventional sources of Fe on pot marigold (*Calendula officinalis* L.) plants symbiotically with arbuscular mycorrhizal (AM). Pot marigold plants were inoculated with *Funneliformis mosseae* in addition to applying ferrous sulfate, FeNPs, and Fe-EDDHA at a rate of 10 mg Fe/kg soil, which follows the recommended rates of fertilizer. Their effects on plant growth, morphology, and physiological parameters were to be compared in the experiment. According to the findings, FeNPs significantly increased plant height, mean stem length, flower number, and total flower lifespan, especially when used with AMF. Most notably, this treatment produced the highest total chlorophyll content (6.62 mg/g FW), active iron in leaves (10 µg/g FW), essential oil (5.75%), mean number of leaves per plant (26.25), number of flowers per plant (6.5), and overall flower lifespan (92.75 days). It also produced superior mycorrhizal root colonization (52.47%). However, because of its lower uptake efficiency and rapid oxidation, ferrous sulfate showed limited performance. By enhancing iron bioavailability, the FeNPs promoted more effective metabolic activity and nutrient absorption. These results demonstrate the advantage of producing FeNPs as a bio-sustainable and biocompatible alternative for synthetic chelates, thus providing an interesting way to improve crop growth promotion in mycorrhizal cropping systems.

Keywords Arbuscular mycorrhizal fungi, Fertilizer, Iron nanoparticles, Plant growth, Pot marigold

*Correspondence:
Elham Malekzadeh
emalekzadeh@gau.ac.ir
[1]Department of Soil Science, Faculty of Water and Soil Engineering, Gorgan University of Agricultural Sciences and Natural Resources, PO Box: 4918943464, Gorgan, Golestan Province, Iran
[2]Department of Cellulose Science and Engineering, Faculty of Wood and Paper Engineering, Gorgan University of Agricultural Sciences and Natural Resources, Gorgan, Iran

Introduction

Pot marigold (*C. officinalis* L.) is a medicinal plant widely recognized for its pharmacological properties, including anti-inflammatory [1, 2], antibacterial [3], antiparasitic activity [4], and wound-healing effects [5]. It is rich in bioactive compounds such as flavonoids, carotenoids, and essential oils, which contribute to its therapeutic potential [6, 7]. Due to its wide applications in the pharmaceutical, cosmetic, and agricultural industries, optimizing its growth and biochemical composition is of great significance [8–11].

The growth of pot marigold is highly dependent on the environment and the nutrients it receives, especially iron (Fe), which is essential for healthy plant development [12–14]. Iron plays an important role in plant metabolism and is involved in enzymatic reactions, electron transport, and chlorophyll synthesis [15, 16]. If plants do not receive enough iron, their growth and productivity are severely impaired, as iron is crucial for processes such as photosynthesis, respiration, and nitrogen fixation [15, 17]. Although iron is abundant in the soil, plants often have difficulty absorbing it as it tends to form insoluble compounds, especially in neutral to alkaline soils [15]. This leads to iron deficiency, which results in yellowing leaves (chlorosis), poor photosynthesis, stunted growth and lower crop yields [13, 18]. Farmers usually use synthetic Fe fertilizers such as Fe chelates (Fe-EDTA and Fe-DTPA) or Fe sulfate to remedy this deficiency [16, 19]. But these fertilizers have their downsides such as they oxidize quickly, can be easily washed out, and can even harm the environment. Too much iron can also become toxic and disrupt the delicate balance of nutrients in plant cells and the soil microbiota [20].

Iron oxide nanoparticles (FeNPs) have emerged as a promising solution for addressing Fe deficiency in plants and improving seed germination [13, 21–24]. Due to their nanoscale dimensions, high surface area, and unique physicochemical properties, FeNPs exhibit superior Fe solubility and controlled release, facilitating efficient uptake and utilization by plants [25–27]. Several studies have demonstrated that FeNPs can enhance chlorophyll synthesis, promote root elongation, and improve overall plant performance under Fe-deficient conditions [13, 21–24, 28–30]. Compared to conventional Fe fertilizers, FeNPs minimize nutrient loss through leaching and reduce environmental risks [31, 32]. However, the method of FeNPs synthesis significantly influences their bioavailability, stability, and potential toxicity [13].

Conventional methods for synthesizing FeNPs (such as chemical and physical approaches) often come with major advantages [33]. They typically rely on hazardous chemicals, consume high energy, and produce toxic by-products, making them less than ideal for sustainable agriculture [34, 35]. In contrast, green synthesis has gained traction as an eco-friendly alternative, utilizing biological molecules from leaf extract [36], tea extract [37], flower extract [38], agricultural waste extract [39], root extract [40], vegetable and fruit peel extracts [41], papermaking waste and nanocellulose [13], egg peel extract [42], microorganisms [43, 44], or seaweed polysaccharides [45] to facilitate nanoparticle formation. Among these biomaterials, nanocellulose has emerged as a highly effective stabilizing and reducing agent for metal nanoparticle synthesis [13, 46–49]. Nanocellulose, a renewable and biodegradable nanostructured polymer derived from plant biomass, possesses remarkable physicochemical properties such as high surface area, functional hydroxyl (OH) groups, and excellent biocompatibility [50–53]. These attributes serve as an effective matrix for stabilizing metal nanoparticles, preventing their agglomeration, and enhancing their bioavailability in soil–plant systems. Moreover, using nanocellulose for the synthesis or bio-templates of nanoparticles eliminates the need for hazardous reducing agents [48], aligning with the principles of green chemistry and sustainable development.

The effectiveness of FeNPs in improving plant nutrition largely depends on their uptake mechanisms or FeNPs-plants [54, 55]. Several pathways have been proposed for FeNPs internalization, including root absorption via apoplastic and symplast pathways [56, 57] and foliar penetration through leaf epidermis or stomata [58]. Studies suggest that FeNPs can undergo dissolution and act as nano-nutrients for plants, releasing Fe ions that are subsequently assimilated through conventional Fe transporters [16, 21–23, 55, 58, 59]. Additionally, FeNPs may be internalized as intact particles, accumulating in internal organelles or chloroplasts and causing damage. However, factors such as nanoparticle size, surface charge, and coating materials influence their uptake efficiency and physiological effects. Understanding these mechanisms is crucial for optimizing FeNPs formulations for agricultural applications.

In addition to Fe supplementation, beneficial soil microorganisms play a critical role in nutrient acquisition and plant health [60]. AM fungi form symbiotic associations with plant roots, facilitating nutrient absorption, improving water uptake, and enhancing stress tolerance [61–67]. AM fungi contribute to Fe bioavailability, secreting chelating compounds, and promoting root system expansion [68]. AM fungi promote iron and nutrient uptake in host plants by increasing the effective soil volume that roots can access via their extensive hyphal networks. The AM fungi also promote the natural production of phytosiderophores in the host plant to increase the solubility and mobility of Fe in the rhizosphere. AM fungi can also exude low-molecular-weight organic acids (citric acid and oxalic acids) that 'mobilize'

insoluble forms of Fe in the soil, or induce expression of high-affinity iron transporters in plant roots to enhance the acquisition of Fe [69]. Not only does AM fungi augment iron uptake, but it also increases plant tolerance to stressful conditions (drought, salinity) or heavy metals. AM fungi are capable of improving drought, salinity, and heavy metal tolerance by increasing plants' ability to uptake nutrients and water, boosting antioxidants, regulating hormones, and supporting photosynthesis and biomass production. AM fungi also promote resilience in ecosystems through enhanced soil structures, nutrient cycling, and carbon retention [70]. Despite the potential benefits, limited studies have explored the combined impact of AM and FeNPs on medicinal plants like pot marigold plants.

While FeNPs have been researched extensively in agricultural applications, there are still gaps in our knowledge regarding the potential of NC-assisted green synthesis of FeNPs and their interactions with medicinal plants and symbiotic fungi. Most of the previous research has centered on chemically synthesized FeNPs, which are environmentally hazardous as they contain toxic remnants and unstable formulations. Further, though FeNPs have been reported to improve plant growth and metabolism, the function of nanocellulose as a novel and sustainable stabilizing and reducing agent in FeNP synthesis is yet to be explored. Despite the well-known significance of AMF in improving nutrient acquisition and stress tolerance, the synergistic interactions among AM and FeNPs in medicinal plants such as pot marigold remain less investigated. This study bridges these research gaps by demonstrating a green, nanocellulose-mediated method for FeNP synthesis that offers higher biocompatibility, controllable release, and minimal impact on environmental pollution. Moreover, it also provides novel insights regarding the tripartite interaction between nanocellulose-assisted FeNPs, AM (*F. mosseae*), and pot marigold and their synergistic effects on the physiology, essential oil composition, and productivity of the plant. The results of this work will aid in the design of sustainable nano-fertilization processes, as well as contribute towards the research of clean agriculture and the cultivation of medicinal plants.

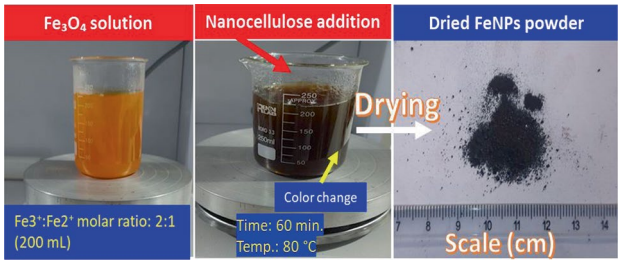

Fig. 1 The color change in the suspension of FeNPs during synthesis

Materials and methods

Materials

The pot marigold seeds were purchased from Pakan Seed Company in Isfahan, Iran. The main reagents used in this study included iron chloride in two forms: ferric chloride ($FeCl_3{\cdot}6H_2O$) and ferrous chloride ($FeCl_2{\cdot}4H_2O$), both of analytical grade with 99% purity, and sodium hydroxide (NaOH) supplied by Merck (Darmstadt, Germany). Fe-EDDHA (iron ethylenediamine-N, N'-bis(2-hydroxyphenylacetic acid)) with 6% iron content was purchased from Scharlau (Barcelona, Spain). Additionally, agriculture ferrous sulfate monohydrate fertilizer ($FeSO_4{\cdot}H_2O$) with 18% iron content was obtained from Merck (Darmstadt, Germany).

Preparation of AM (*F. mosseae*)

The arbuscular mycorrhizal (AM) fungus used in this study (*F. mosseae*) was obtained from Turan Biotech Co. (Semnan Science & Technology Park, Iran), a certified provider of microbial inoculants. Fungal spores were extracted using the wet sieving technique and counted using a binocular microscope (ZSM-1001), revealing an inoculum potential of 150 viable spores per 100 g of inoculum based on the number of healthy spores [71, 72].

Preparation of nanocellulose

Nanocellulose was produced using a super disk grinder (MKCA6-2; Masuko Sangyo Co., Ltd., Japan) through a mechanical process. A 1% (w/v) cellulose suspension obtained from bleached softwood kraft pulp was prepared in deionized water and subjected to grinding at 1500 rpm. The grinding process was carried out in multiple passes, gradually reducing the gap between the rotating and stationary disks to enhance fibrillation. This mechanical treatment resulted in the formation of a stable nanocellulose gel (2.5 wt%), which was then stored at 4 °C for further analysis and applications [73, 74].

Green synthesis of fenps with nanocellulose

During the synthesis of FeNPs, a nanocellulose gel at a concentration of 15% (relative to the total weight of $FeCl_3$) was introduced into a 100 mL solution of Fe_3O_4 (0.1 M) and maintained at 80 °C for 60 min. Following this step, 120 mL of NaOH (1.0 M) was added while vigorously stirring the mixture mechanically. The rapid appearance of a black coloration signified the successful reduction of FeNPs, as illustrated in Fig. 1.

Characterization of nanocellulose and fenps

Field emission scanning electron microscopy (FESEM) and energy dispersive X-ray analysis (EDX)

Field emission scanning electron microscopy (FESEM) was employed to examine the morphological characteristics of nanocellulose and FeNPs. The FeNPs, separated

via high-speed centrifugation, and the nanocellulose gel were dried in a drying oven (Memmert UNB-500, Germany) at 60 °C for 24 h to achieve a constant weight. The dried samples were then coated with a platinum layer (< 0.2 nm) using a sputter coater (Quorum, Q150R ES, UK) under vacuum. Subsequently, the coated specimens were analyzed using a FESEM (MIRA3, TESCAN-XMU, Czech Republic) equipped with an energy-dispersive X-ray spectrometer (SAMx Numerix, Levens, France) at an accelerating voltage of 10 kV.

Transmission electron microscopy (TEM)

The morphology of the synthesized FeNPs was analyzed using transmission electron microscopy (TEM) (Zeiss EM10, Oberkochen, Germany). For this purpose, aqueous suspensions containing 0.01 wt% of FeNPs were carefully deposited onto a nickel grid coated with Formvar© polymer. The samples were then allowed to dry at room temperature to ensure complete evaporation of the solvent. TEM imaging was carried out at an accelerating voltage of 1.5–5 kV, enabling high-resolution visualization of the nanostructures.

Table 1 The physicochemical properties of the soil

Properties	Unit	Value	Method
Textural class	-	Loam-clay	Hydrometer method
pH	-	7.18	pH meter (pH 700 benchtop meter, Oakton) in saturated soil paste
Electrical conductivity (EC)	dS/m	0.81	EC meter (Hanna Instruments, Model HI5321-02) in saturated soil paste
Saturation percentage (SP)	%	56.04	Gravimetric method
Organic carbon (OC)	%	1.0	Walkley–Black method
Total nitrogen (N)	%	0.06	Kjeldahl method
Calcium carbonate content	%	27.12	Back-titration the excess acid with NaOH.
Available phosphorus (P)	mg/kg	9.0	Olsen method with extraction by sodium bicarbonate
Available potassium (K)	mg/kg	201.5	The atomic absorption spectrometer method, extracted by 1 N ammonium acetate
Available iron (Fe)	mg/kg	2.47	The atomic absorption spectrometer method, extracted by DTPA
Available zinc (Zn)	mg/kg	0.11	
Available copper (Cu)	mg/kg	0.43	
Available manganese (Mn)	mg/kg	3.64	

Size distribution analysis

The size distribution of nanocellulose and synthesized FeNPs was analyzed by Digimizer image analysis software (version 4.1.1.0; MedCalc Software, Mariakerke, Belgium). The nanocellulose and FeNPs were calibrated using a nanoscale microscope, revealing these very high-resolution images. For nanocellulose, 100 particles and for FeNPs, 300 particles were manually drawn and measured their diameters. Histograms were generated from exported data that showed the characteristics of the size distribution of FeNPs. Statistical parameters were calculated to gain insight into the particle size distribution, including mean size and standard deviation.

Zeta potential

Zeta potential was measured with a dynamic light scattering (DLS) spectrometer with electrophoretic light scattering function (Zetasizer Nano, Malvern, UK). The nanoparticle suspension was diluted previously with deionized water at suitable concentrations to dismiss multiple scattering effects and avoid too low signal intensity. Each sample was measured in triplicate and presented as the mean ± standard deviation.

Experimental design

The physicochemical characteristics of the soils are displayed in Table 1. The planter soil was sterilized immediately before planting (121 °C for 60 min.) to minimize the contribution of native soil microorganisms and ensure were measuring only the symbiotic effects of AM fungi. It can conclude then that indigenous microbial communities (pseudomonas and others) were also eliminated with this sterilization process, including bacteria capable of producing siderophores, which can be a major environmental determinant of iron in the rhizosphere. The experiment treatments involved the application of 10 mg/kg synthesized FeNPs, iron sulfate 18%, and Fe-EDDHA 6% (based on fertilizer recommendation of 10 mg Fe/kg soil). During the emergence and germination test, 10 seeds were sown evenly at a depth of 3 cm. After thinning, four plants were left in each pot (Fig. 2). The pots used in this experiment measured 16 cm in diameter and 15 cm in height, providing adequate volume (2 kg) for plant growth under controlled conditions. After counting the number of spores, the *F. mosseae* fungus inoculum was inoculated as a thin layer at a distance of 1 cm below the seeds. The plants were then housed under controlled conditions in a growth room with a temperature of 28 ± 1 °C, a light cycle of 16 h, and an 8-hour dark period. Humidity was maintained at 80% of field capacity (FC).

Determination of plant morphological properties

To assess the growth characteristics of pot marigold, several variables were measured at the flowering stage

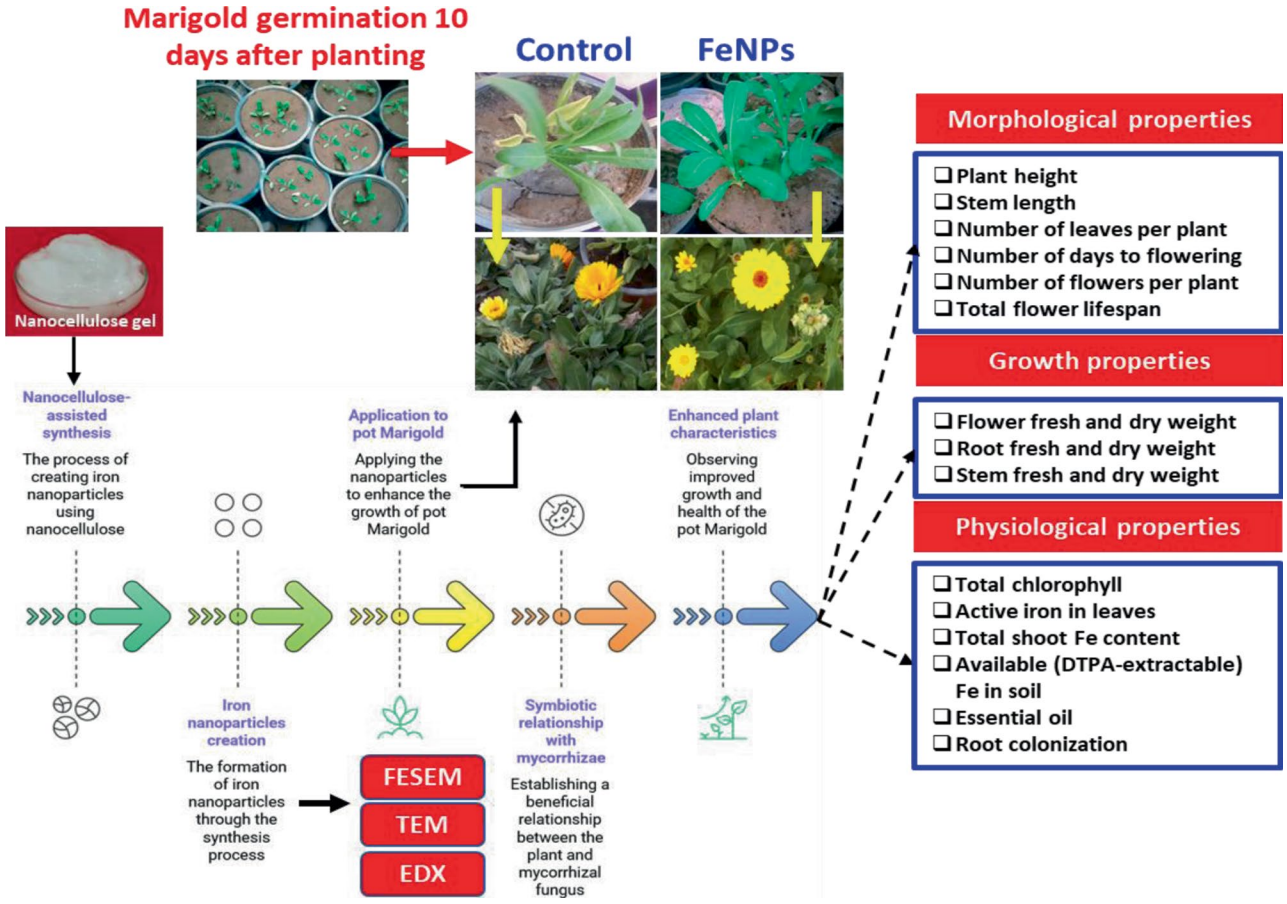

Fig. 2 Schematic of experimental treatments in this study

using morphological parameters. For plant height and stem length, a digital caliper was used to measure from the base of the plant to the highest point of the plant and stem, respectively. The time from sowing to harvesting the plant was 150 days, which was from March to July. The first flower appeared at 40–45 days after sowing, and the flowers were counted and monitored continually until the end of a 150-day cultivation period to account for any drop-off in the number of flowers. The number of leaves and the number of flowers were counted by hand per plant [75, 76]. The total flower lifespan was determined by monitoring the time from flower opening to wilting.

Determination of plant growth properties

Fresh and dry weights of different plant parts, including flower, root, and stem, were measured using a digital analytical balance. Fresh weight was recorded immediately after harvesting, while dry weight was determined after drying the samples in an oven at 70 ± 2 °C until a constant weight was achieved [77, 78].

Total chlorophyll content

The total chlorophyll content can be determined using the Dixit, Rani and Kumar [79] method. Fresh leaf tissue (0.1 g) is homogenized in 10 mL of 80% acetone and centrifuged at 10,000 rpm for 10 min to obtain a clear supernatant. The absorbance of the supernatant is measured at 645 and 663 nm using a spectrophotometer. All steps should be performed under low-light conditions to prevent chlorophyll degradation. The total chlorophyll content (chl *a* + chl *b*) is calculated using Eq. 1:

$$\begin{aligned} &\mathrm{Total chlorophyll\,(mg/gFW)} \\ &= 20.2\,(\mathrm{A_{645}}) + 8.02\,(\mathrm{A_{663}}) \\ &\times\,([\mathrm{V}/1000] \times \mathrm{W}) \end{aligned} \tag{1}$$

where A645 and A663 are the absorbance values at the respective wavelengths, V is the final volume of extract (mL), and W is the fresh weight of the sample (g).

Fe determination

Total shoot Fe content was determined using an atomic absorption spectrophotometer (AAS) (model AA-6300, Shimadzu, Japan) after digestion with nitric acid-perchloric acid [59]. Available (DTPA-extracta) iron in soil was extracted using DTPA (diethylenetriaminepentaacetic acid) and quantified via AAS (model AA-6300, Shimadzu, Japan) [80]. Active iron in leaves was measured

using the ortho-phenanthroline method after extraction with 0.1 N HCl [81].

Essential oils extraction

Extraction of essential oils from pot marigold flowers was carried out using a Clevenger apparatus based on the procedure described by Ahmed, Seleiman [82] and Jaimand, Bagher Rezaee and Homami [83] with a slight modification. A 0.1 g of dried flowers was extracted in 10 mL distilled water by the hydro-distillation method for 3 h. The essential oil was dried over anhydrous sodium sulfate and then stored in sealed, dark vials at 4 °C for further studies [84]. Essential oil was calculated as the ratio of extracted essential oil to the dry weight of the flower (Eq. 2).

$$Essential\ oil\ (\%) = \frac{EW}{DM} \times 100 \quad (2)$$

Root colonization assessments

Root staining was performed based on the procedure described by Sun and Tang [85] with a slight modificationTrypan blue staining was employed to prepare root samples for subsequent assessment of AMF colonization. The roots were sectioned into 1 cm fragments and subjected to a sequential processing procedure: clearing in 10% hot KOH at 60 °C for 60 min, softening in an alkalized H_2O_2 solution for 20 min, acidification with 5% lactic acid for 3 min, staining overnight with a 0.05% trypan blue solution, and finally destaining using a lactic acid–glycerin mixture (1:1, v/v) at room temperature. The stained roots were examined under a dissecting stereo microscope (Olympus SZ61, 40× magnification), where both vertical and horizontal gridlines were systematically scanned, recording the presence or absence of fungal infection at each intersection point. Each root segment was analyzed four times by repositioning the samples. The percentage of colonization was determined by dividing the number of intersections showing AM fungal structures by the total number of root–grid intersections examined.

Statistical analysis

The outcomes of each section were presented as mean ± standard deviation (SD). Statistical analysis was conducted using SPSS software (version 20, SPSS Inc., Chicago, USA). A completely randomized design (CRD) with four replications per treatment was used for the experiment. Analysis of variance (ANOVA) was performed to assess statistical significance, and mean comparisons were conducted using Duncan's multiple range test (DMRT) at significance levels of $P < 0.05$ and $P < 0.01$.

Results

Nanocellulose characterization

Figure 3 illustrates the characterization results of nanocellulose. The digital photograph (Fig. 3a) depicts a highly viscous nanocellulose gel at a concentration of 2.5 wt%, which is attributed to its extensive nanofiber network and high specific surface area. FESEM micrographs, along with diameter distribution analysis, confirm that the nanocellulose exhibits nanoscale dimensions, with an average diameter of 35.05 ± 6.67 nm and lengths exceeding 10 µm (Fig. 3b, c). The zeta potential (ζ) of the nanocellulose suspension was measured at − 31.7 ± 1.69 mV, indicating good colloidal stability due to sufficient surface charge, which effectively prevents particle aggregation through electrostatic repulsion. The positive or negative values higher than ± 30 mV are considered stable dispersal [86, 87]. This level of stability is favorable for its role as a dispersing or stabilizing agent in nanoparticle formulations. EDX analysis showed that the nanocellulose contained 53.1 wt% carbon, 2.01 wt% nitrogen, and 44.89 wt% oxygen (Fig. 3d).

FeNPs characterization

The characterization of FeNPs was carried out using advanced techniques, including TEM, FESEM, EDX, and particle size distribution analysis (Fig. 4). TEM analysis showed that the FeNPs exhibited a spherical morphology with an average particle size of < 100 nm. FESEM micrograph showed that the particles had a uniform distribution, good dispersion, or relative agglomeration tendency. The presence of agglomeration was observed, with particles grouped in clusters of > 200 nm. This suggests that the nanoparticles may exhibit strong inter-particle interactions. EDX analysis confirmed the presence of Fe in the nanoparticles, with the characteristic peaks corresponding to Fe, O, C, etc. The atomic ratio of Fe was calculated to be 7.05%, confirming the successful synthesis of FeNPs. The elemental composition was consistent with the green synthesis method. Particle size distribution analysis showed a narrow distribution with a peak size of 25.4 ± 2.12 nm. This indicates that the majority of the nanoparticles are within the range of 10–40 nm, which suggests a uniform particle size ideal for fertilizer applications.

The synthesized FeNPs exhibited a polydispersity index (PDI) of 0.197, indicating a narrow particle size distribution and a high degree of uniformity among the nanoparticles. According to established criteria, PDI values less than 0.3 typically reflect a good monodisperse system with well-dispersed particles [88], which is desirable for applications requiring consistent behavior and predictable interactions in biological or soil environments. Furthermore, the measured zeta potential (ζ) of − 33.3 ± 2.12 mV shows that the FeNPs possessed a sufficiently high

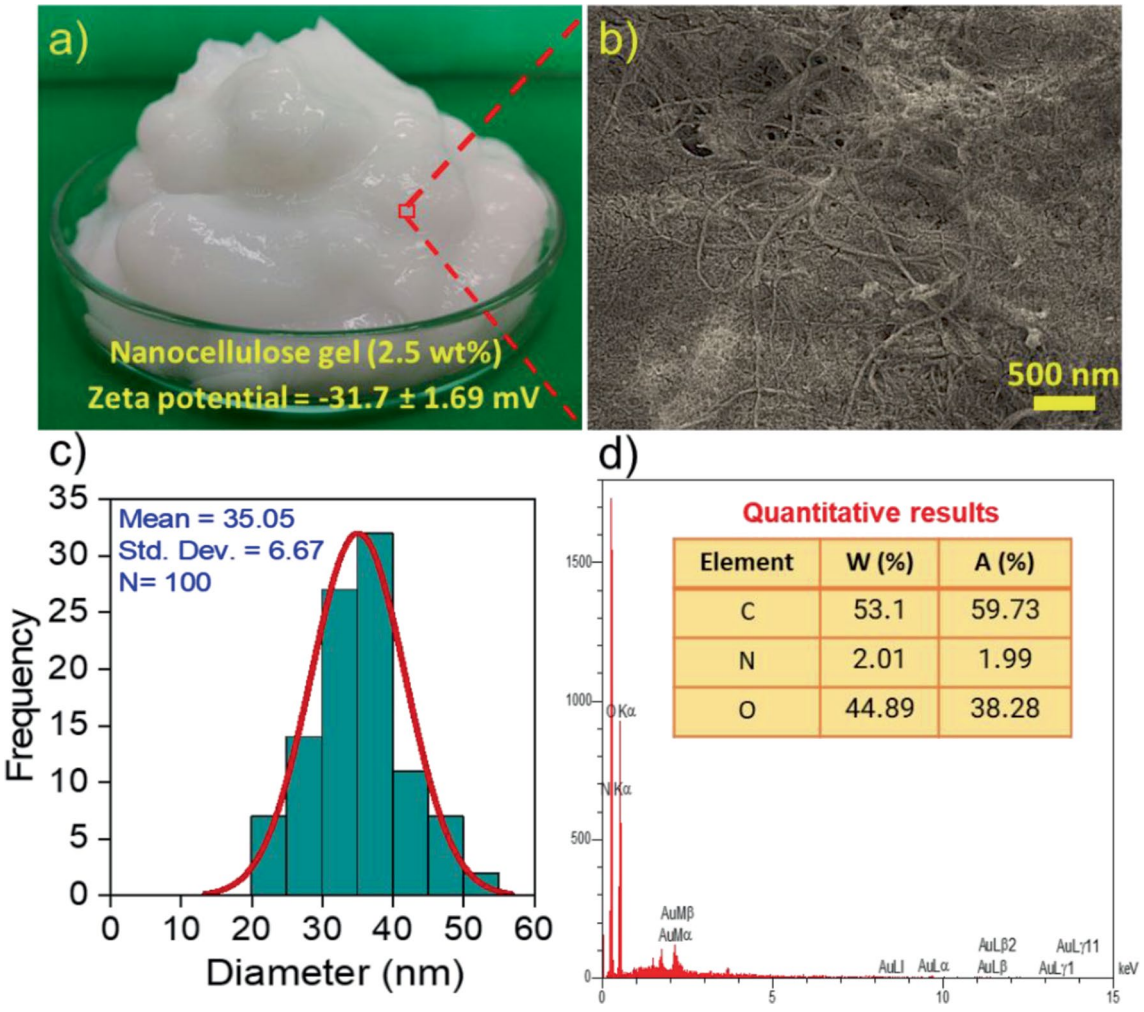

Fig. 3 Nanocellulose characterization: **a**) digital photograph of nanocellulose gel with a concentration of 2.5 wt% alongside their value of zeta potential, **b**) FESEM micrograph of nanocellulose, **c**) diameter distribution analysis, and **d**) EDX analysis

surface charge to maintain colloidal stability in aqueous suspension. Zeta potentials exceeding ± 30 mV are typically considered for a good stable colloidal dispersion, which minimizes agglomeration and sedimentation [86, 87].

Effects of different fertilizer treatments on morphological parameters

The results of the analysis of variance (ANOVA) presented in Table 2 show the effects of different fertilizer treatments on various morphological parameters of the plants. Significant differences were observed at the 1% level for most parameters, including plant height (94.31), mean stem length (43.87), mean number of leaves per plant (45.54), number of flowers per plant (2.85), and total flower lifespan (229.2). These results suggest that the fertilizer treatments had a considerable effect on these parameters. However, the number of days to flowering did not show a significant difference ($p > 0.05$), suggesting that the timing of flowering was not strongly influenced by the fertilizer treatments.

The effect of different iron treatments, including FeNPs, ferrous sulfate, and Fe-EDDHA, on the morphological parameters of pot marigold compared to the control treatment is provided in Fig. 5. The results showed that plants treated with FeNPs + AM fungi exhibited the greatest improvements in plant height (44.25 cm; Fig. 5a), mean stem length (24 cm; Fig. 5b), number of leaves per plant (26.25; Fig. 5c), number of flowers per plant (6.5; Fig. 5e), and total flower lifespan (92.75 days; Fig. 5f). Similarly, the Fe-EDDHA + AM fungi significantly (Duncan's test, $^{**}p < 0.01$) enhanced plant height (45 cm; Fig. 5a), mean stem length (23.25 cm; Fig. 5b), and total flower lifespan (85.5 days; Fig. 5f) compared to other treatments. Across all fertilization treatments, AM fungal inoculation consistently promoted plant growth relative to non-mycorrhizal counterparts (Duncan's test, $^{**}p < 0.01$). Figure 5g shows morphological changes in the

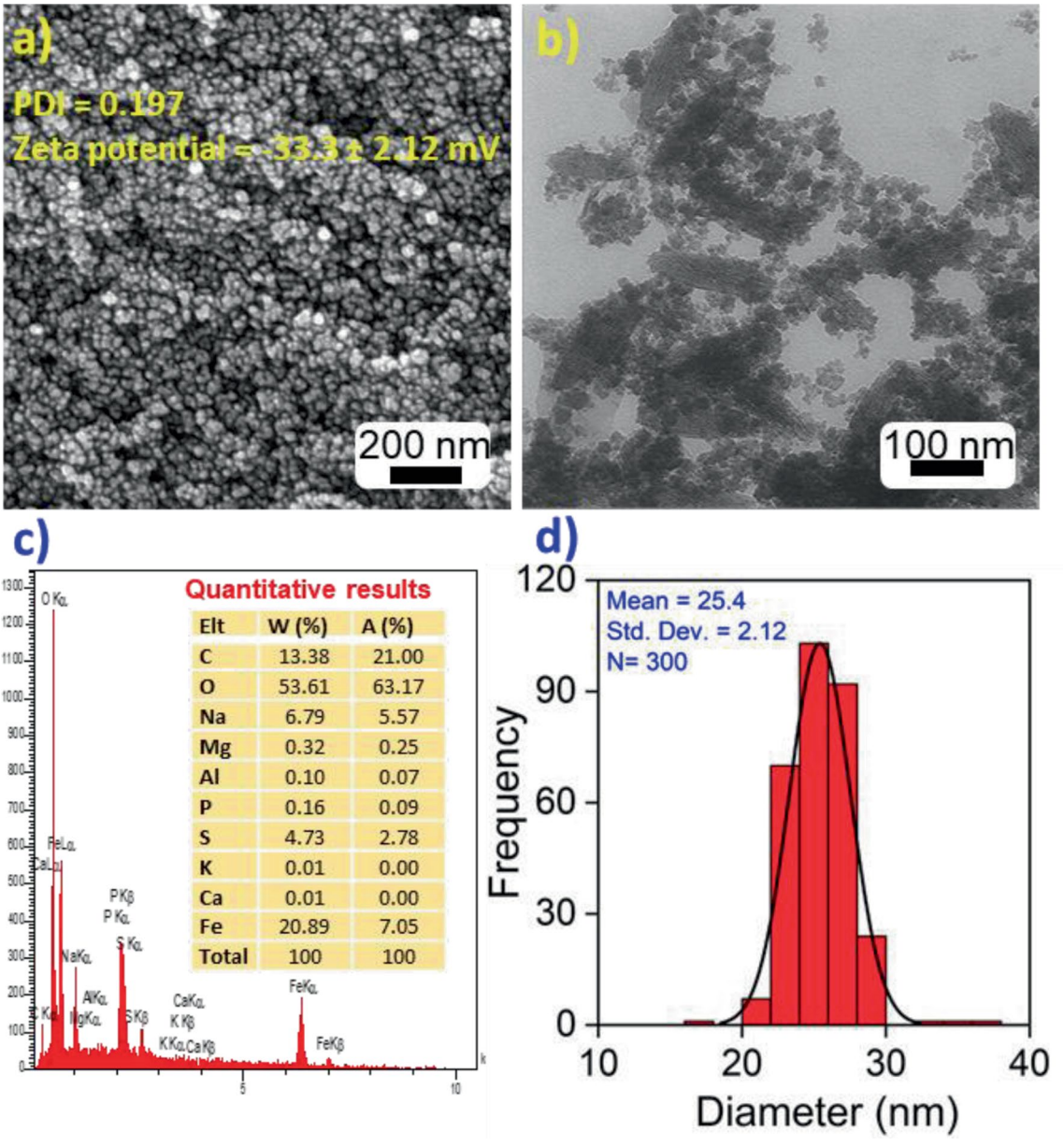

Fig. 4 FeNPs characterization: **a**) FESEM micrograph, **b**) TEM micrograph, **c**) EDX analysis, and **d**) diameter distribution analysis

Table 2 Analysis of variance (ANOVA) results for the effects of different fertilizer treatments on morphological parameters

SOV	df	Mean square (MS)					
		Height	Mean stem length	Mean number of leaves per plant	Number of days to flowering	Number of flowers per plant	Total flower lifespan (days)
Treatment	7	94.310**	43.871**	45.539**	7.929ns	2.853**	229.246**
Error	24	2.825	1.951	4.681	23.417	0.427	14.052
Total	31	97.135	45.822	50.22	31.346	3.28	243.298

**: Significant difference at 1% level; ns: non-significant

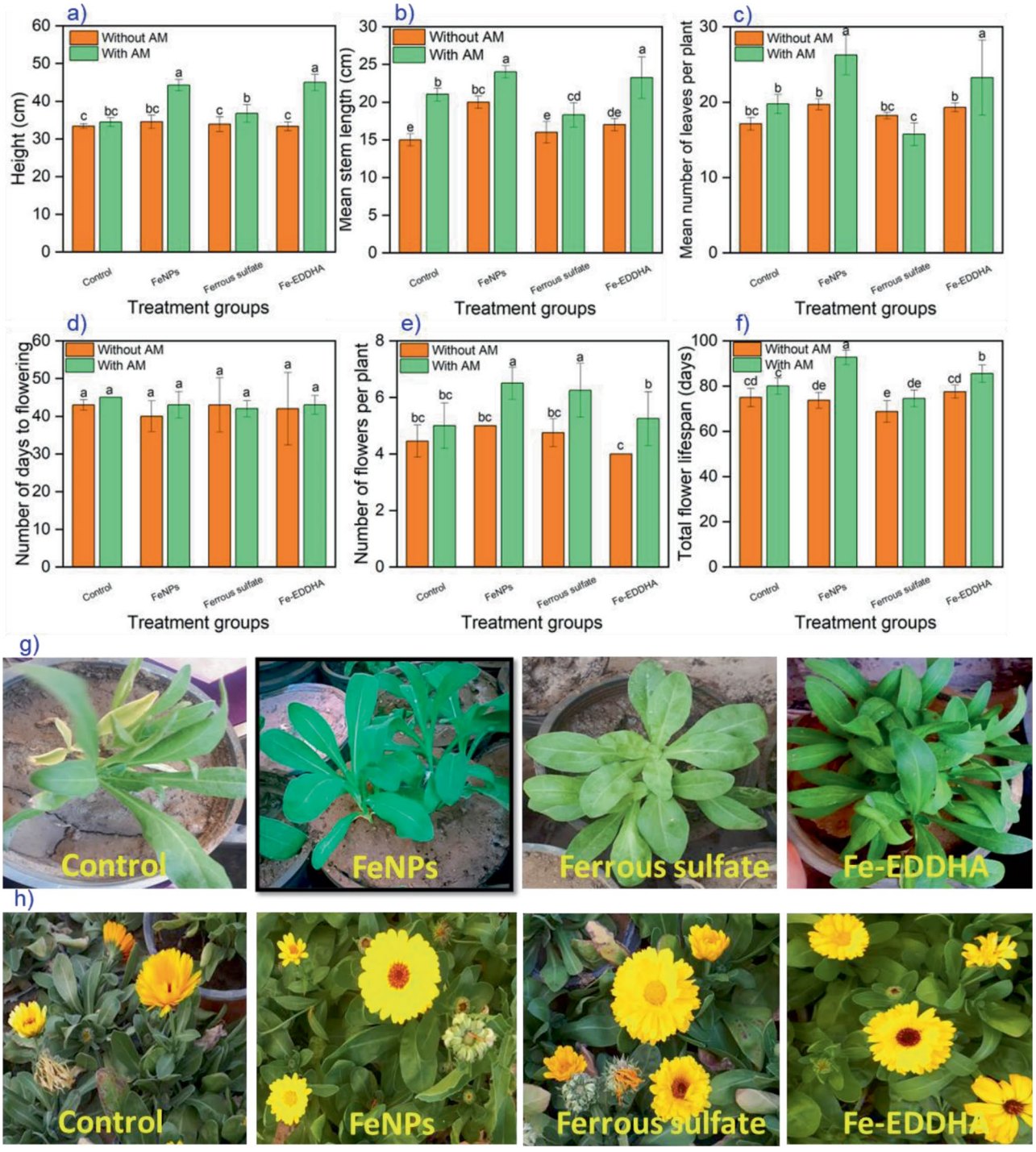

Fig. 5 Effects of different fertilizer treatments on plant morphological parameters: **a**) height, **b**) mean stem length, **c**) mean number of leaves per plant, **d**) number of days to flowering, **e**) number of flowers per plant, **f**) total flower lifespan, **g**) morphological changes in the pre-flowering stage, and **h**) plants conditions after flowering

pre-flowering stage, while Fig. 5h shows the plant's conditions after flowering. The results indicate that FeNPs and Fe-EDDHA treatments enhanced leaf density and improved flowering compared to the control. Plants treated with FeNPs and Fe-EDDHA lead to larger flowers with more intense yellow pigmentation, whereas control plants exhibited stunted growth and leaf chlorosis.

Effects of different fertilizer treatments on growth parameters

The ANOVA results showed significant differences (**$p < 0.01$) in all growth parameters, including flower fresh and dry weight, root fresh and dry weight, and stem fresh and dry weight, under different fertilizer treatments (Table 3).

Figure 6 shows the growth parameters of pot marigold under different fertilization treatments. The study also revealed that the combined application of FeNPs + AM fungi significantly increased growth parameters over all other treatments (Duncan's test, **$p < 0.01$). The highest flower fresh and dry weights (1.37 g and 0.462 g, Fig. 6a, b) and root fresh and dry weights (4.02 g and 1.47 g, respectively; Fig. 6c, d), as well as stem biomass (1.12 g and 0.3 g, Fig. 6e, f) were observed in the FeNPs + AM fungi treatments. Conventional Fe sources, including ferrous sulfate and Fe-EDDHA, also improved growth compared to the control, but their effects were less pronounced than FeNPs, particularly in the presence of AM fungi.

Effects of different fertilizer treatments on physiological parameters

The ANOVA results presented in Table 4 show significant differences (**$p < 0.01$) in all physiological parameters, including total chlorophyll, active iron in leaves, total shoot iron content, available (DTPA-extractable) iron in soil, and essential oil content, under the different fertilizer treatments. The physiological characteristics of pot marigold under various fertilization treatments are presented in Fig. 7. The use of different sources of iron, especially in combination with AM fungi, had a strong impact on the physiological aspects of pot marigold. The treatment FeNP + AM had the highest total chlorophyll (6.62 mg/g FW), which was a 57.6% increase for the control (4.2 mg/g FW), and a 27.3% increase above the control + AM (5.2 mg/g FW) (Fig. 7a). The FeNP + AM treatment had the highest active iron concentration in the leaves at 10 µg/g FW or 170.3% and 100% above the control (3.7 µg/g FW) and control + AM (5.0 mg/g FW), respectively (Fig. 7b). Similarly with total shoot Fe content at 415.25 µg/g FW with FeNP + AM application, which was a 77.1% enhancement compared to control (234.5.0 µg/g FW) and a 22.9% increase over control + AM (337.75 µg/g FW) (Fig. 7c). The highest available iron in soil (9.0 mg/kg) was also observed in FeNP + AM of 54.6% and 21.3% increase from respect control treatments (Fig. 7d). The essential oil content of pot marigold increased to 5.75% in the FeNP + AM reflect an increase of 283.3% compared to control (1.5%) and a 27.8% increase compared to control + AM (4.5%) (Fig. 7e).

Root colonization

Table 5 shows the percentage of root colonization by *F. mosseae* in pot marigold plants under different iron fertilizer treatments (FeNPs, ferrous sulfate, and Fe-EDDHA), both with and without AM fungi. Root colonization was absent in all treatments without AM fungi, confirming the specificity of the symbiotic interaction. Among AM-inoculated treatments, the highest colonization (52.47%) was observed in the FeNP + AM, significantly exceeding other treatments based on Duncan's test. The Fe-EDDHA + AM and ferrous sulfate + AM treatments showed moderate colonization levels of 47.85% and 45.70%, respectively, while the AM-inoculated control exhibited the lowest colonization (43.90%) among the AM-treated groups. Analysis of variance (ANOVA) revealed a highly significant treatment effect ($F = 519.579$, $P < 0.001$), confirming that the type of iron fertilizer significantly influences mycorrhizal colonization when AM fungi are present. The root colonization results are presented in Fig. 8. In the control group (without AM fungi), the pictures show roots with no fungal colonization structures. This will illustrate that there was no AM fungi interaction, where no AM fungi were applied (Fig. 8a). No colonization with roots was observed for

Table 3 Analysis of variance (ANOVA) results for the effects of different fertilizer treatments on growth parameters

SOV	df	Mean square (MS)					
		Flower fresh weight /plant	Flower dry weight /plant	Root fresh weight /plant	Root dry weight /plant	Stem fresh weight /plant	Stem dry weight /plant
Treatment	7	0.120**	0.037**	0.976**	0.434**	0.087**	0.026**
Error	24	0.012	0.001	0.018	0.027	0.013	0.001
Total	31	0.132	0.038	0.994	0.461	0.10	0.027

**: Significant difference at 1% level

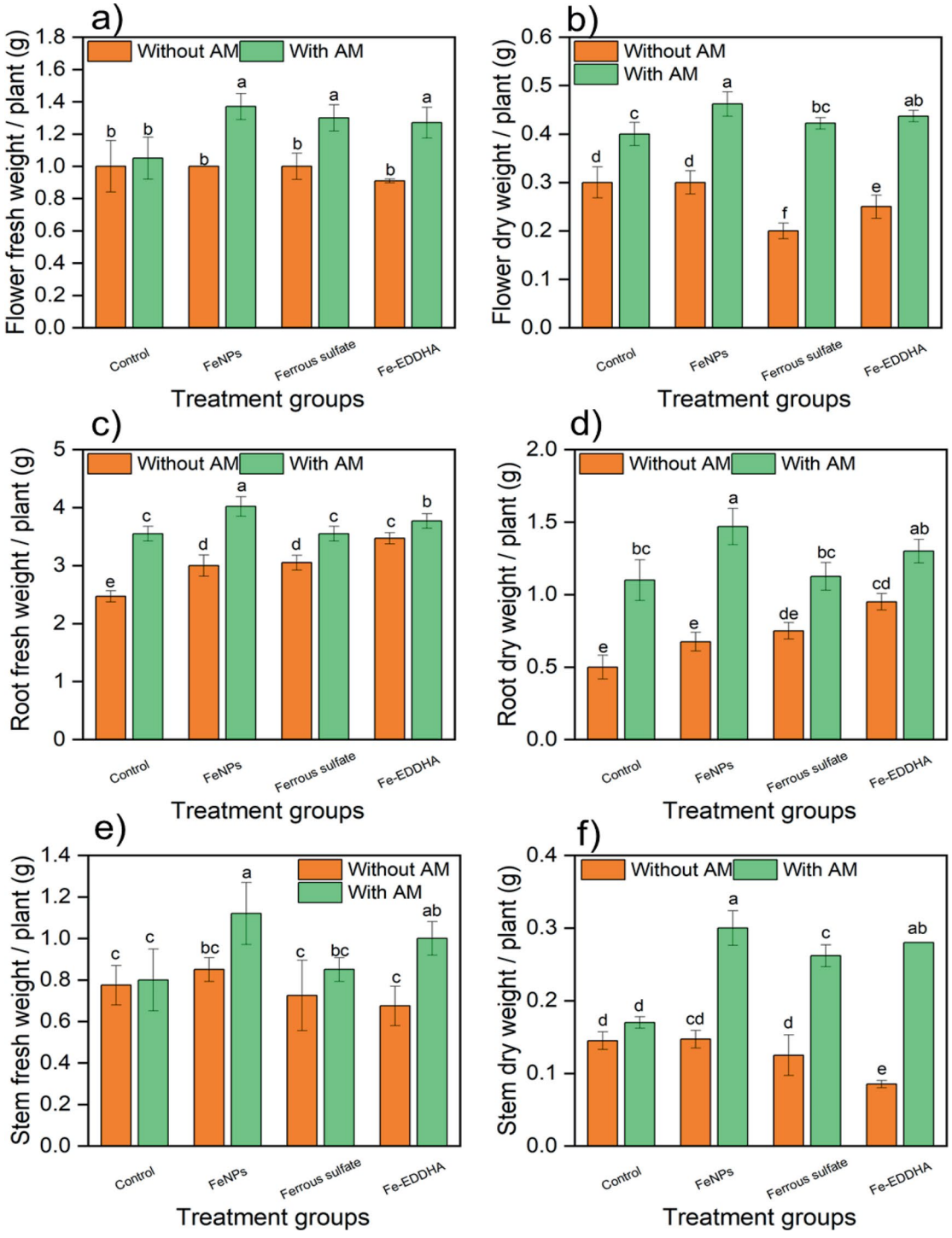

Fig. 6 Effects of different fertilizer treatments on plant growth parameters: **a**) flower fresh weight, **b**) flower dry weight, **c**) root fresh weight, **d**) root dry weight, **e**) stem fresh weight, and **f**) stem dry weight

all treatments without AM fungi to confirm that without AM fungi, no colonization would occur. In contrast, images from treatments with AM fungi would display fungal structures on the roots, indicating successful colonization (Fig. 8b). The FeNPs + AM fungi treatment, with the highest colonization rate of 52.47%, would likely show the most extensive fungal growth on the roots, suggesting that the presence of FeNPs facilitates a more effective symbiotic relationship between the roots and AM fungi (Fig. 8c, d). The ferrous sulfate + AM fungi and Fe-EDDHA + AM fungi treatments, with colonization rates of 45.70% and 47.85%, respectively (Fig. 8e, f), would also

Table 4 Analysis of variance (ANOVA) results for the effects of different fertilizer treatments on physiological parameters

SOV	df	Mean square (MS)				
		Total chlorophyll	Active iron in leaves	Total shoot Fe content	Available (DTPA-extractable) Fe in soil	Essential oil
Treatment	7	2.409**	17.014**	20011.638**	7.061**	10.734**
Error	24	0.080	0.346	454.323	0.289	0.127
Total	31	2.489	17.36	20465.961	7.35	10.861

**: Significant difference at 1% level

exhibit fungal structures on the roots, but these might be less abundant or less densely distributed compared to FeNPs.

Correlation analysis

The heatmap-cluster analysis reveals significant correlations among plant growth, physiological, and metabolic traits, with values ranging from −0.01 to +1 (Fig. 9). Strong positive correlations were found between the height and stem dry weight ($r = 0.839$), as well as between root colonization and total shoot Fe content ($r = 0.885$), indicating that more root colonization can increase the iron-uptake ability. Of note, essential oil content correlates highly with root colonization ($r = 0.937$) and total shoot Fe content (**$r = 0.932$), suggesting that nutrient supplementation could influence secondary metabolite production and/or vice versa. In contrast, number of days to flowering shows little or even inverse correlation with almost all parameters, except for fresh weight of flowers (r = -0.012) and active iron in leaves ($r = 0.025$), signifying that the delayed cycle of flowering does not necessarily result in enhanced biomass accumulation or absorption of iron. The clustering analysis additionally encompasses closely related variables into clusters, where the flower and root biomass parameters forming variables were most condensed into a cluster, illustrating their partnership in plant productivity. Moreover, active iron is strongly correlated with chlorophyll content in leaves ($r = 0.677$), further affirming the role of iron in photosynthesis. These findings indicate significant synergistic interactions promoting plant growth and suggest that proper iron nutrition, specifically in the context of root colonization, not only increases plant growth but also essential oil yield in pot marigold.

Discussion

The effect of FeNPs on plant growth and development largely depends on the method of application of FeNPs, their size, and plant species [89–93]. FeNPs, due to their small size, exhibit enhanced absorption efficiency by plant roots, facilitated by their increased surface area-to-volume ratio, resulting in improved nutrient uptake under low concentration [13, 94]. The improved iron availability from FeNPs and conventional sources of Fe supports enhanced chlorophyll synthesis and photosynthetic efficiency [95], thereby promoting vegetative growth and flowering. The observed enhancements in plant morphology can be attributed to the synergistic interaction between AM fungi and iron fertilization. AM fungi are known to facilitate nutrient and water uptake by extending the root surface area through extraradical hyphae, which is particularly beneficial for phosphorus and iron acquisition.

The superior performance of FeNPs + AM compared to other treatments suggests that FeNPs provide a more controlled and sustained release of iron, thereby preventing deficiencies and promoting prolonged metabolic activity, ultimately delaying senescence. In contrast, ferrous sulfate, despite being a readily available iron source, exhibited lower efficacy in enhancing growth, possibly due to its rapid oxidation and reduced bioavailability in soil. The observed increases in flowering and extended flower longevity under AM fungal inoculation highlight its crucial role in alleviating oxidative stress, improving nutrient acquisition, and enhancing plant resilience, ultimately leading to superior physiological performance. These results were in close agreement with the findings of Sun, Qu [94], who reported that the use of FeNPs has improved the growth characteristics and chlorophyll content of *Kobresia capillifolia* seedlings. Elfeky, Mohammed [91] reported that the application of 3.0 mg/L FeNPs in soil had a suitable effect in improving the growth and yield of basil plants. In another study, it was reported that the application of 50, 100, and 200 mg/L of nano-silicon increased the growth characteristics of pot marigold plants [2].

The FeNPs improve nutrient uptake more effectively than Fe-EDTA through several interrelated mechanisms rooted in their nanoscale properties and release dynamics. FeNPs are a more stable and organized type of iron than Fe-EDTA, which is subject to rapid leaching in some soil situations and can maintain availability in the rhizosphere for longer periods [95]. This fact of the sustained release reduces the leaching of iron, or precipitation fixation, of the iron, especially in alkaline or calcareous soils when Fe-EDTA becomes ineffective. The high surface reactivity, higher dose, and small particle size of nanoparticles facilitate closer interactions with plants, enhancing their bioavailability and uptake efficiency [96]. In contrast, Fe-EDTA does not exhibit such stimulatory effects and may even interfere with microbial activity due to its synthetic nature. Zia-ur-Rehman, Mfarrej [95]

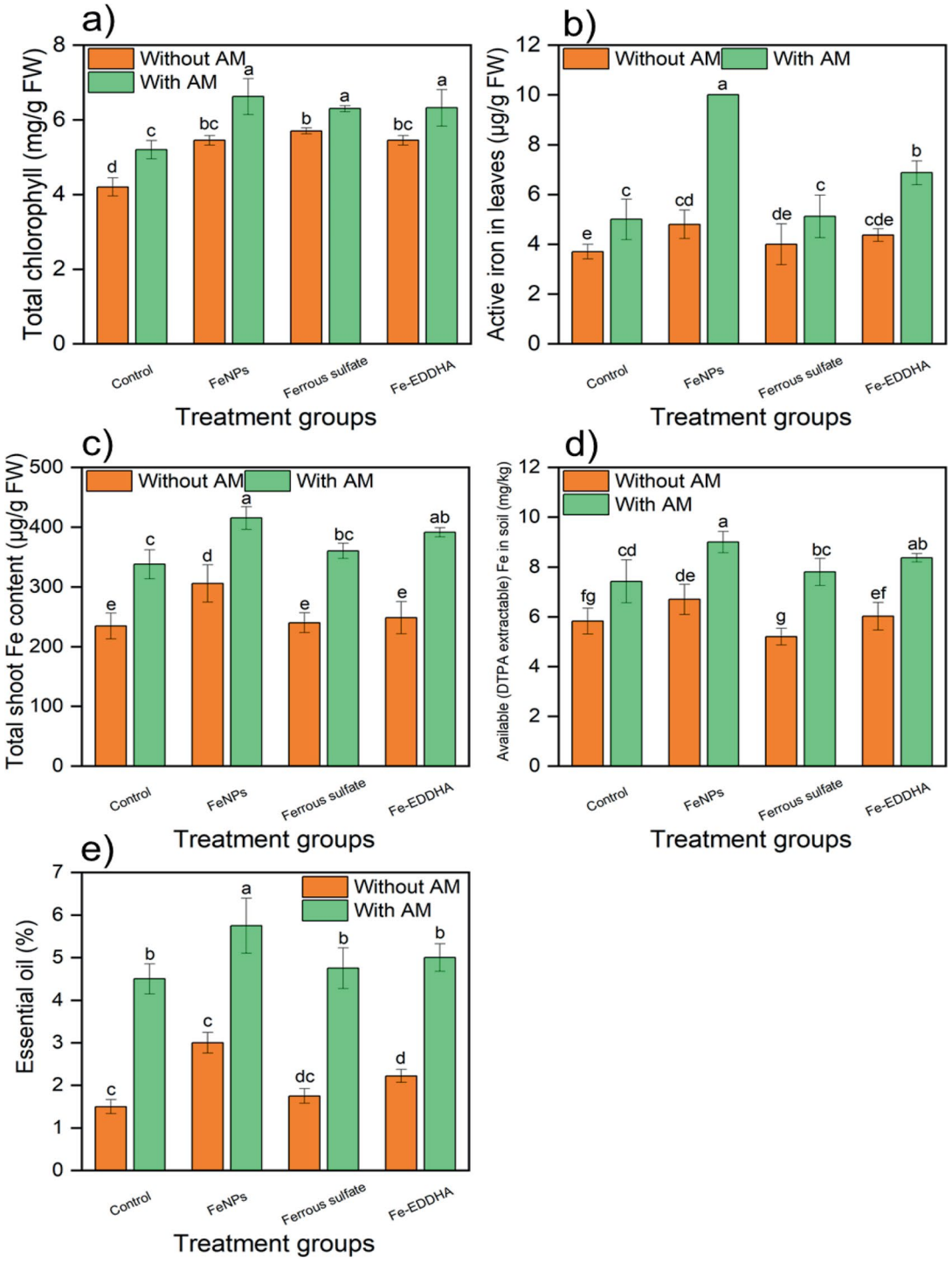

Fig. 7 Effects of different fertilizer treatments on plant physiological parameters: **a**) total chlorophyll, **b**) active iron in leaves, **c**) total shoot Fe content, **d**) available (DTPA extractable) Fe in soil and **e**) essential oil content

observed that FeNPs increased the assimilation of essential nutrients, Fe, Zn, Ca, Mg, and K, and also increased the dry weights of the roots, shoots and grains more than Fe-EDTA, specifically in salt-stressed and normal soils. Tung, Phong [97] reported that FeNPs led to higher chlorophyll content and antioxidant enzyme activity (SOD and APX) than Fe-EDTA in *Chrysanthemum morifolium* plants, supporting better stress tolerance and photosynthesis. In carnation plantlets, the addition of FeNPs raised root formation, antioxidant enzyme activity (superoxide dismutase, catalase, and ascorbate peroxidase), and

Table 5 Root colonization of pot marigold by *F. mosseae* under different iron fertilizer treatments with and without AM fungi, along with ANOVA and Duncan's test results

Treatment groups	AM fungi	Root colonization (%)	Duncan test
Control	Without AM	0	d
	With AM	43.90	c
FeNPs	Without AM	0	d
	With AM	52.47	a
Ferrous sulfate	Without AM	0	d
	With AM	45.70	bc
Fe-EDDHA	Without AM	0	d
	With AM	47.85	b
Analysis of variance (ANOVA) results for root colonization.			
SOV	**df**	***F*-value**	***P*-value**
Treatment	7	519.579	< 0.001
Error	24	5.004	
Total	31		

overall mineral absorption compared to Fe-EDTA, indicating a higher level of nutrient bioavailability [98].

The FeNPs have been shown to stimulate root morphological traits and promote AM colonization, both of which contribute to improved growth parameters [99, 100]. Singh, Chauhan [66] found that inoculation of AM fungi (*F. mosseae* and *R. intraradices*) improved the growth, reproductive characteristics and bioactive compounds of tomato plants. In another study, Singh and Singh [67] reported that AM fungi can improve the growth characteristics and photosynthetic yield of tomato plants under both irrigation and drought stress conditions.

Nanocellulose is essential to enhance the bioavailability of FeNPs and support their functionality with AM fungi. This background allows for the dispersal of nanoparticles and prevents aggregation, as well as mitigates the release in the rhizosphere. It is a non-toxic environment for living organisms, with its structure breaking down and being biodegradable, therefore creating a non-toxic environment for microbes to interact with. This promotes AM development and provides a positive microbial environment around the roots. FeNPs and AM can synergistically improve iron usage in a few ways in a two-part approach: AM develops greater root surface area with hyphae and releases siderophores to sequester Fe, while FeNPs provide a steady supply of the usable Fe^{3+}. Altogether, increase plant uptake, transfer, and use of iron. This method increases basic and essential life processes

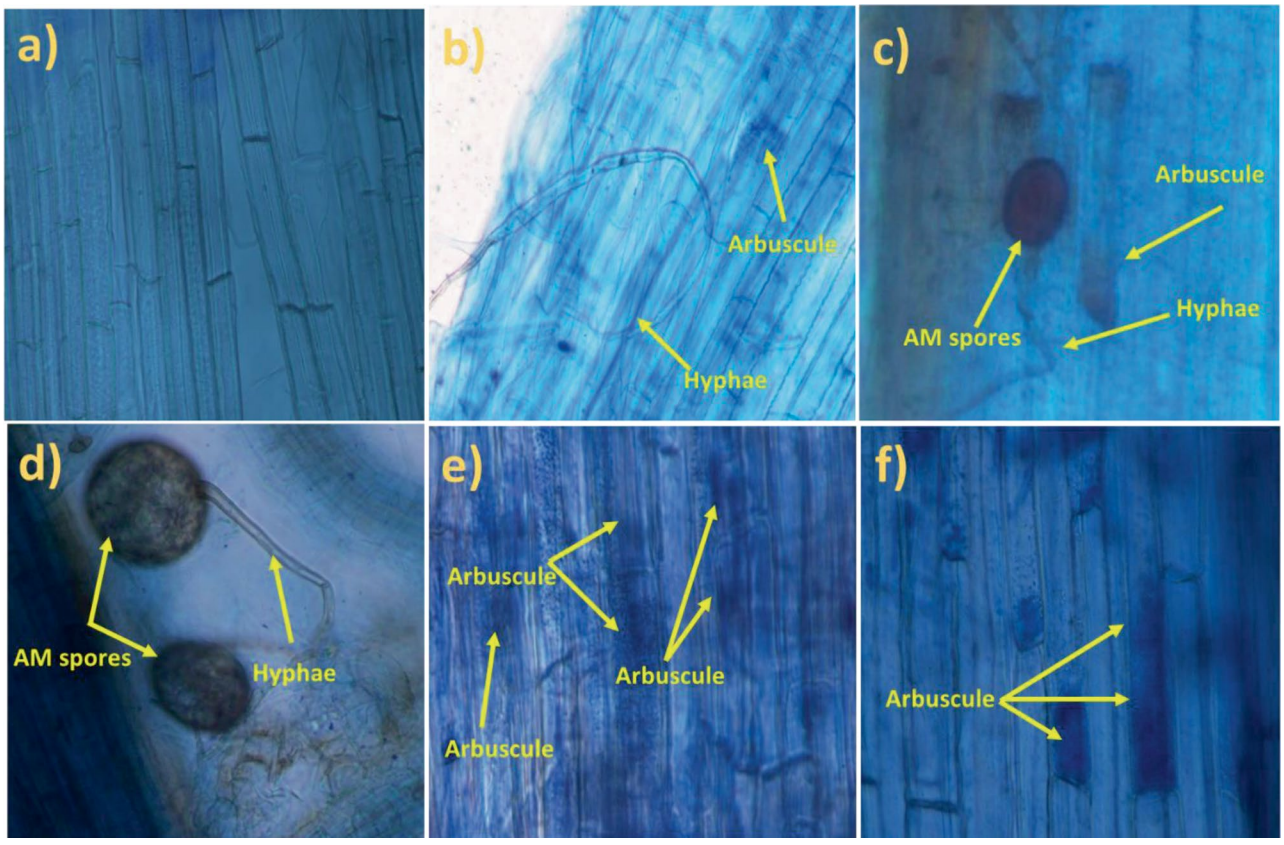

Fig. 8 Root colonization by AM fungi (magnification level = 40X): **a**) control-without AM, **b**) control + AM, **c**,**d**) FeNPs + AM, **e**) ferrous sulfate + AM, and **f**) Fe-EDDHA + AM

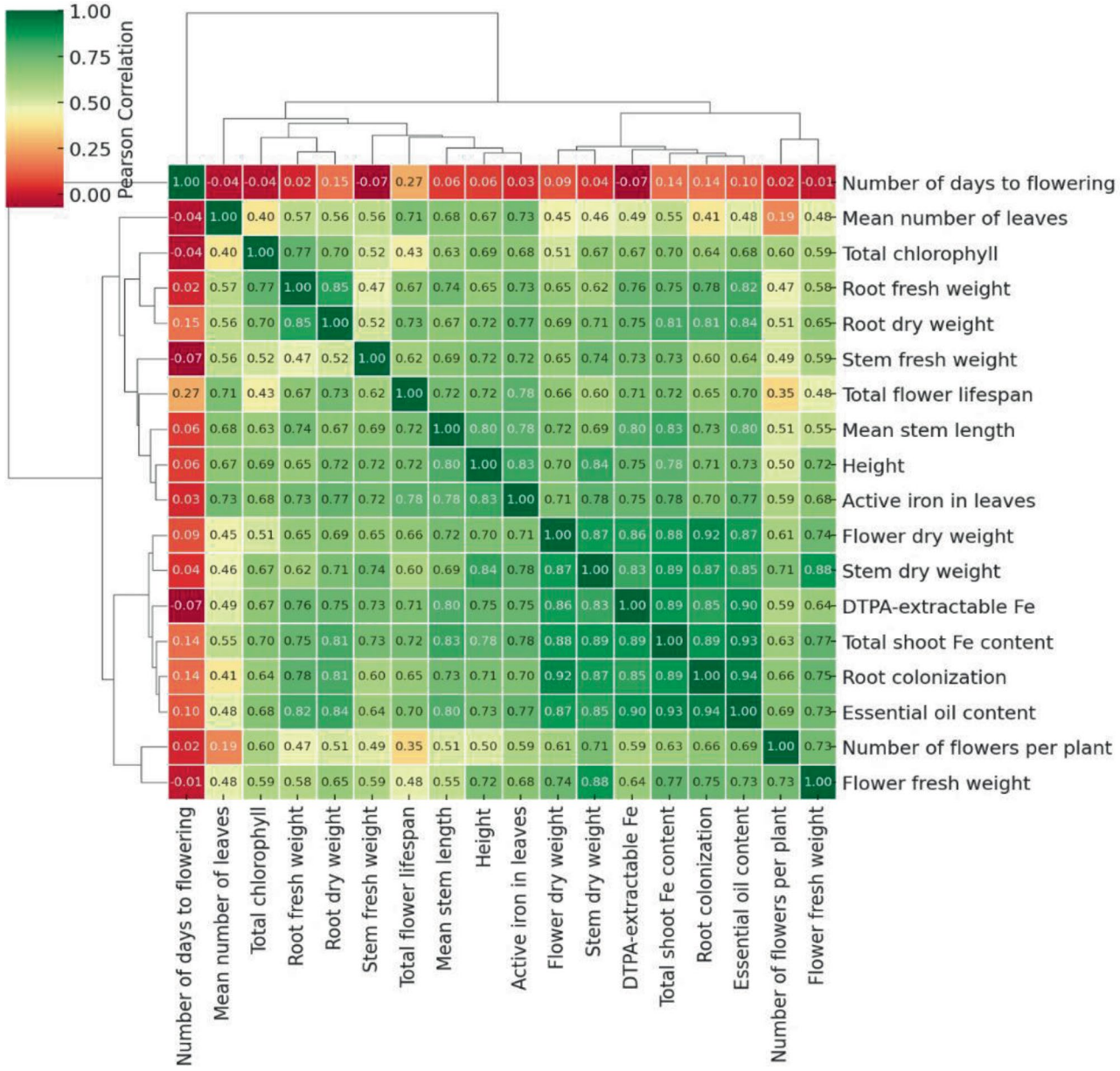

Fig. 9 The heatmap-cluster analysis of the Pearson's correlation coefficient for morphological, growth, and physiological parameters of pot marigold

and also encourages plants to produce additional beneficial compounds, such as essential oils and flavonoids. Typically and generally, this occurs as a part of plant support systems through a more robust way of managing stress through medicinal plants.

The results of this study revealed that FeNPs, especially in association with mycorrhizae, improved growth parameters of plants considerably higher than conventional Fe sources, indicating greater bioavailability and uptake of FeNPs. Synergistic interactions between the FeNPs and the *F. mosseae* could exert an effect that promotes the solubility of the FeNPs and their transport in the plant system, consequently increasing root and shoot biomass production. Notably, the root weight was higher in FeNPs + AM treatment, suggesting that due to mycorrhizal colonization, the root system was more developed, leading to more uptake of nutrients. Furthermore, the increase in flower biomass in this treatment indicates that FeNPs promote vegetative growth in addition to reproductive success, which are both important for the medicinal and ornamental value of pot marigold. Moreover, soil supplementation with traditional Fe sources (Fe-EDDHA and ferrous sulfate) promoted moderate plant growth; however, their effects were significantly weaker than those in the case of the bacterium, probably associated with their lower mobility and availability

in the rhizosphere. Thus, the diminished efficacy of these treatments in the absence of AM stresses the critical role of fungal symbiosis in improving Fe use efficiency.

In comparison, while FeNPs alone also improved chlorophyll and iron content, the addition of AM fungi resulted in further increases in these parameters. Ferrous sulfate treatments with AM inoculation also enhanced physiological traits, including chlorophyll and iron content, but to a lesser extent than FeNPs + AM. The lowest physiological response was observed in the control and ferrous sulfate treatments without AM fungi, where chlorophyll content, active iron in leaves, and essential oil production were comparatively low. The observed improvements in physiological parameters, especially in plants treated with FeNPs and AM fungi, can be attributed to the synergistic effects between the mycorrhizal fungi and the iron sources. Zia-ur-Rehman, Mfarrej [95] reported that with the application of FeNPs (15 and 25 mg/kg soil), the total chlorophyll content of wheat plants increased by 23.2 and 38.4%, respectively, compared to the control treatment. Also, the application of Fe-EDTA and ferrous sulfate increased the total chlorophyll content of the plant compared to the control. Kanjana [101] reported that with the application of iron nanoparticles (nano-Fe_3O_4), the chlorophyll content of cotton plants increased by 4.01% compared to the control treatment. Rui, Ma [59] reported that the application of 10 mg/kg of FeNPs increased the amount of chlorophyll compared to the control treatment. The increase in active iron in leaves and total shoot iron content under FeNPs + AM treatment suggests that the nano ferric particles facilitated a controlled and sustained release of iron, making it more readily available for plant uptake. Increased Fe in plants has been reported with the application of FeNPs in cucumber [102], wheat [95], basil [91], *Citrus maxima* seedlings [54], peanut [59], *Capsicum annuum* [103], sunflower [89], and rice [104].

Enhancing the chlorophyll content and plant growth characteristics could increase the production of essential oils in aromatic and medicinal plants. Iron may have a similar effect on the biosynthesis of secondary metabolites as stress signals, which could increase the production of these compounds [92]. The higher essential oil content under FeNPs + AM treatments indicates improved metabolic activity and secondary metabolite production, potentially driven by enhanced nutrient and iron availability. In contrast, the relatively lower responses in treatments with ferrous sulfate, especially without AM fungi, may be due to the rapid oxidation and limited availability of iron in the soil, which may not be efficiently absorbed by the plants. An increase in essential oil content has been reported with the use of iron nanoparticles in plants such as basil [91], pot marigold [90], and *Dracocephalum kotschyi* [92].

FeNPs could be an economical alternative to conventional iron fertilizers for plant nutrition with potentially lower application rates and higher efficiencies. Traditional iron fertilizers such as Fe-EDDHA, Fe-EDTA, ferrous sulfate, and other unfamiliar fertilizers often have repeated applications in portions of soil testing because of leaching or oxidation to other non-plant-available forms. Since FeNPs may remain stable due to controlled release, there may be an increase in bioavailability and nutrient uptake as well as agricultural outcomes (decreased leaching and oxidation). Less input can lead to decreased losses overall and improved agronomic efficiency (greater yield per amount applied). Furthermore, while the FeNPs can be more costly (especially original high-purity or "green-synthesized" formulations), there may be positive environmental, plant, and profitability benefits to employing FeNPs in terms of crop performance throughout the growing season to offset a higher initial expense. Many of these benefits help facilitate sustainable agriculture and environmental stewardship. Therefore, purchasing FeNPs versus a traditional commercially available iron fertilizer may be valuable.

Limitations, future prospects, and policy implications of fenps for plant growth

Although FeNPs have incredible potential, their use within the agriculture field is limited for a variety of reasons. One of the more fundamental problems is the stability of nanoparticles in plants, with the FeNPs being particularly prone to oxidation and agglomeration in solution, which will hinder their bioavailability for plant uptake. Factors such as species selection, soil conditions, and environmental conditions can also create variability in plant response, making more widespread applications challenging. In general, the stability of FeNPs in the plant rhizosphere is expected to vary over time, with nanoparticles potentially maintaining their bioactivity for several days to weeks, depending on these variables. There are also concerns about toxicity and legacy effects on ecology, as excessive accumulation of nanoparticles in soil and plant tissues can disrupt microbial communities and affect nutrient cycling. Additionally, their high production costs and the requirement for specific synthesis methods reduce their scalability and feasibility, especially in low-resource agricultural systems. The absence of standardized regulations and safety guidelines for FeNP application is another obstacle to successful commercialization.

To overcome these challenges, future research should focus on green synthesis approaches, such as nanocellulose-assisted FeNPs, to enhance biocompatibility and environmental safety. FeNPs stability and nutrient release can be enhanced using controlled-release formulations and coatings. Furthermore, comprehending

plant–microorganism interactions in environments amended with FeNPs, notably in complex symbiotic systems such as AMF, might elucidate mechanisms for enhancing the uptake of plant nutrients. Nano-based precision agriculture methods such as smart nanofertilizers and sensor-based monitoring may further enhance the site-specific delivery of FeNPs, which would minimize wastage and concerns about environmental exposure. To fill the knowledge gaps that currently exist, long-term field experiments, formulation optimization, and multidisciplinary studies that couple nanotechnology with plant physiology and soil science will be essential.

Policymakers need to develop regulatory frameworks for the environmentally safe utilization of FeNPs in agriculture that will address toxicity thresholds and permissible application rates of FeNPs. As a result, standardized risk assessment protocols for assessing the soil-plant bioavailability and transformation of FeNPs are warranted. Sustainability can be improved with the use of nanocellulose in nanoparticle synthesis and policies that encourage eco-friendly nanomaterial production. Additionally, more public awareness and farmer education programs are urgently needed to ensure the safe and efficient adoption of FeNP-enabled fertilizers. Utilizing FeNPs as biofortifying agents can support national and international agricultural and food security agendas through sustainable intensification without creating environmental trade-offs.

Conclusions

The results showed that the FeNPs provided a promising new biocontrol mechanism to combat Fe deficiency and act as a sustainable alternative to traditional Fe fertilizers, especially when paired with AM fungi. FeNPs were responsible for prolonged Fe release, plant height, flowering, and physiological traits enhancement, and improved root colonization. Ferrous sulfate was widely available, but the speed at which it oxidized meant it lacked long-term effectiveness. While AM fungi had positive effects on nutrient uptake, it may have limited biomass accumulation in some treatments due to competition for resources. The better plant performance in FeNPs indicates the provision of appropriate nutrient availability, which maintains the plant-microorganisms interactions. Overall, FeNPs, more pronounced with AM fungi, represent a sustainable strategy to augment plant growth and productivity in agriculture.

Acknowledgements
The content presented in this article has been extracted from the Master's Thesis of Mrs. Maryam Nohesara. The authors gratefully acknowledge support from the Gorgan University of Agricultural Sciences and Natural Resources (9931343008, No. 502-1402.04.24).

Author contributions
M.N: Methodology, Data curation, and Supervision. E.M: Conceptualization, Methodology, Validation, Investigation, Data curation, Writing– review & editing. M.B.M: Methodology, Resources, and Supervision. A.T: Software, Visualization, Resources, Formal analysis, Writing– original draft, Writing– review & editing, and Supervision. All authors read and approved the final manuscript.

Funding
The authors received no financial support for the research, authorship, and/or publication of this paper.

Data availability
The data provided in this study are available to the corresponding author and can be presented on request.

Declarations

Ethics approval and consent to participate
All methods performed in this study complied with the relevant institutional, national, and international guidelines and legislation.

Consent for publication
Not applicable.

Competing interests
The authors declare no competing interests.

Received: 9 April 2025 / Accepted: 21 May 2025
Published online: 28 May 2025

References

1. Villanueva-Bermejo D, Vázquez E, Villalva M, Santoyo S, Fornari T, Reglero G, Rodriguez Garcia-Risco M. Simultaneous supercritical fluid extraction of Heather (*Calluna vulgaris* L.) and marigold (*Calendula officinalis* L.) and anti-inflammatory activity of the extracts. Appl Sci. 2019;9(11):2245.
2. Eghlima G, Mohammadi M, Ranjabr M-E, Nezamdoost D, Mammadov A. Foliar application of nano-silicon enhances drought tolerance rate of pot marigold (*Calendula officinalis* L.) by regulation of abscisic acid signaling. BMC Plant Biol. 2024;24(1):1220.
3. Vella FM, Pignone D, Laratta B. The mediterranean species *Calendula officinalis* and *Foeniculum vulgare* as valuable source of bioactive compounds. Molecules. 2024;29(15):3594.
4. Băieş M-H, Cotuţiu V-D, Spînu M, Mathe A, Cozma-Petruţ A, Bocăneţ Vl, Cozma V. Satureja hortensis L. and *Calendula officinalis* L., two Romanian plants, with in vivo antiparasitic potential against digestive parasites of swine. Microorganisms. 2023;11(12):2980.
5. Nicolaus C, Junghanns S, Hartmann A, Murillo R, Ganzera M, Merfort I. In vitro studies to evaluate the wound healing properties of *Calendula officinalis* extracts. J Ethnopharmacol. 2017;196:94–103.
6. Dhingra G, Dhakad P, Tanwar S. Review on phytochemical constituents and Pharmacological activities of plant *Calendula officinalis* Linn. Biol Sci. 2022;2(2):216–28.
7. AshwlayanVD KA, Verma M. Therapeutic potential of *Calendula officinalis*. Pharm Pharmacol Int J. 2018;6(2):149–55.
8. Akhtar G, Faried HN, Razzaq K, Ullah S, Wattoo FM, Shehzad MA, et al. Chitosan-induced physiological and biochemical regulations confer drought tolerance in pot marigold (*Calendula officinalis* L). Agronomy. 2022;12(2):474.
9. Król B, Paszko T. Harvest date as a factor affecting crop yield, oil content and fatty acid composition of the seeds of calendula (*Calendula officinalis* L.) cultivars. Ind Crops Prod. 2017;97:242–51.
10. Onofrei V, Teliban G-C, Burducea M, Lobiuc A, Sandu CB, Tocai M, Robu T. Organic foliar fertilization increases polyphenol content of *Calendula officinalis* L. Ind Crops Prod. 2017;109:509–13.
11. Anderson VM, Archbold DD, Geneve RL, Ingram DL, Jacobsen KL. Fertility source and drought stress effects on plant growth and essential oil production of *Calendula officinalis*. HortScience. 2016;51(4):342–8.

12. Izadi Z, Rezaei Nejad A, Abadía J. Physio-morphological and biochemical responses of pot marigold (*Calendula officinalis* L.) to split iron nutrition. Acta Physiol Plant. 2020;42(6):1–14.
13. Malekzadeh E, Tatari A, Motlagh MB, Nohesara M, Mohammadi S. A novel approach for the green synthesis of iron nanoparticles using marigold extract, black liquor, and nanocellulose: effect on marigold growth parameters. Int J Biol Macromol. 2024;267:131552.
14. Saffari VR, Saffari M. Effects of EDTA, citric acid, and tartaric acid application on growth, phytoremediation potential, and antioxidant response of *Calendula officinalis* L. in a cadmium-spiked calcareous soil. Int J Phytoremediation. 2020;22(11):1204–14.
15. Rout GR, Sahoo S. Role of iron in plant growth and metabolism. Reviews Agricultural Sci. 2015;3:1–24.
16. Shirsat S. Iron oxide nanoparticles as iron micronutrient fertilizer—opportunities and limitations. J Plant Nutr Soil Sci. 2024;187(5):565–88.
17. Brear EM, Day DA, Smith PM. Iron: an essential micronutrient for the legume-rhizobium symbiosis. Front Plant Sci. 2013;4(359):1–15.
18. Li J, Cao X, Jia X, Liu L, Cao H, Qin W, Li M. Iron deficiency leads to chlorosis through impacting chlorophyll synthesis and nitrogen metabolism in *Areca catechu* L. Front Plant Sci. 2021;12:710093.
19. Hildebrand M-C, Rebl A, Nguinkal JA, Palm HW, Baßmann B. Effects of fe-dtpa on health and welfare of the African catfish clarias gariepinus (burchell, 1822). Water. 2023;15(2):299.
20. Asati A, Pichhode M, Nikhil K. Effect of heavy metals on plants: an overview. Int J Application or Innov Eng Manage. 2016;5(3):56–66.
21. Bidi H, Fallah H, Niknejad Y, Tari DB. Iron oxide nanoparticles alleviate arsenic phytotoxicity in rice by improving iron uptake, oxidative stress tolerance and diminishing arsenic accumulation. Plant Physiol Biochem. 2021;163:348–57.
22. Shah AA, Yasin NA, Mudassir M, Ramzan M, Hussain I, Siddiqui MH, et al. Iron oxide nanoparticles and selenium supplementation improve growth and photosynthesis by modulating antioxidant system and gene expression of chlorophyll synthase (CHLG) and protochlorophyllide oxidoreductase (POR) in arsenic-stressed *Cucumis melo*. Environ Pollut. 2022;307:119413.
23. Haydar MS, Ghosh S, Mandal P. Application of iron oxide nanoparticles as micronutrient fertilizer in mulberry propagation. J Plant Growth Regul. 2021;41:1726–46.
24. Abdulfatah HF, Abdulrahman MF, Naji EF. Green synthesis of iron nanoparticles to promote seed germination of *Zea mays* under salinity condition. Heliyon. 2025;11(2):e41823.
25. Sharma B, Tiwari S, Kumawat KC, Cardinale M. Nano-biofertilizers as bio-emerging strategies for sustainable agriculture development: potentiality and their limitations. Sci Total Environ. 2023;860:160476.
26. Jampílek J, Kráľová K. Nanomaterials for delivery of nutrients and growth-promoting compounds to plants. In: Prasad R, Kumar M, Kumar V, editors. Nanotechnology: an agricultural paradigm. Singapore: Springer; 2017. pp. 177–226.
27. Arora S, Murmu G, Mukherjee K, Saha S, Maity D. A comprehensive overview of nanotechnology in sustainable agriculture. J Biotechnol. 2022;355:21–41.
28. Cieschi MT, Polyakov AY, Lebedev VA, Volkov DS, Pankratov DA, Veligzhanin AA, et al. Eco-friendly iron-humic nanofertilizers synthesis for the prevention of iron chlorosis in soybean (*Glycine max*) grown in calcareous soil. Front Plant Sci. 2019;10(413):1–17.
29. Kumar P, Kumar SV. Nanopriming of *Eleusine coracana* seeds using phyto-assisted magnetic nanoparticles (Fe_3O_4) synthesized from *Colocasia esculenta* leaves. Biomass Convers Biorefinery. 2024;14(17):21329–43.
30. Shahzad R, Harlina PW, Khan SU, Koerniati S, Hastilestari BR, Ningrum RA, et al. Iron oxide nanoparticles alleviate salt-alkaline stress and improve growth by modulating antioxidant defense system in Cherry tomato. J Plant Interact. 2024;19(1):2375508.
31. Sundararajan N, Habeebsheriff HS, Dhanabalan K, Cong VH, Wong LS, Rajamani R, Dhar BK. Mitigating global challenges: Harnessing green synthesized nanomaterials for sustainable crop production systems. Global Challenges. 2024;8(1):2300187.
32. Wahab A, Muhammad M, Ullah S, Abdi G, Shah GM, Zaman W, Ayaz A. Agriculture and environmental management through nanotechnology: eco-friendly nanomaterial synthesis for soil-plant systems, food safety, and sustainability. Sci Total Environ. 2024;926:171862.
33. Pechyen C, Tangnorawich B, Toommee S, Marks R, Parcharoen Y. Green synthesis of metal nanoparticles, characterization, and biosensing applications. Sens Int. 2024;5:100287.
34. Dikshit PK, Kumar J, Das AK, Sadhu S, Sharma S, Singh S, et al. Green synthesis of metallic nanoparticles: applications and limitations. Catalysts. 2021;11(8):902.
35. Verma C, Verma DK, Berdimurodov E, Barsoum I, Alfantazi A, Hussain CM. Green magnetic nanoparticles: a comprehensive review of recent progress in biomedical and environmental applications. J Mater Sci. 2024;59(2):325–58.
36. Devatha C, Thalla AK, Katte SY. Green synthesis of iron nanoparticles using different leaf extracts for treatment of domestic waste water. J Clean Prod. 2016;139:1425–35.
37. Huang L, Weng X, Chen Z, Megharaj M, Naidu R. Green synthesis of iron nanoparticles by various tea extracts: comparative study of the reactivity. Spectrochim Acta Part A Mol Biomol Spectrosc. 2014;130:295–301.
38. Karpagavinayagam P, Vedhi C. Green synthesis of iron oxide nanoparticles using *Avicennia marina* flower extract. Vacuum. 2019;160:286–92.
39. Pan Z, Lin Y, Sarkar B, Owens G, Chen Z. Green synthesis of iron nanoparticles using red peanut skin extract: synthesis mechanism, characterization and effect of conditions on chromium removal. J Colloid Interface Sci. 2020;558:106–14.
40. Niraimathee V, Subha V, Ravindran RE, Renganathan S. Green synthesis of iron oxide nanoparticles from *Mimosa pudica* root extract. Int J Environ Sustain Dev. 2016;15(3):227–40.
41. Tyagi PK, Gupta S, Tyagi S, Kumar M, Pandiselvam R, Daştan SD, et al. Green synthesis of iron nanoparticles from spinach leaf and banana Peel aqueous extracts and evaluation of antibacterial potential. J Nanomaterials. 2021;2021(1):4871453.
42. Kadhim DA, Abid MA, Salih WM. Development of iron oxide nanoparticles using egg Peel (brown) extract as a useful tool for removing the MB dye. Mater Sci Engineering: B. 2024;300:117104.
43. Mahanty S, Bakshi M, Ghosh S, Chatterjee S, Bhattacharyya S, Das P, et al. Green synthesis of iron oxide nanoparticles mediated by filamentous fungi isolated from Sundarban Mangrove ecosystem, India. BioNanoScience. 2019;9:637–51.
44. Mathur P, Saini S, Paul E, Sharma C, Mehtani P. Endophytic fungi mediated synthesis of iron nanoparticles: characterization and application in methylene blue decolorization. Curr Res Green Sustainable Chem. 2021;4:100053.
45. Kaliaraj GS, Subramaniyan B, Manivasagan P, Kim S-K. Green synthesis of metal nanoparticles using seaweed polysaccharides. In: Venkatesan J, Anil S, Kim S-K, editors. Seaweed polysaccharides: isolation, biological and biomedical applications. Elsevier; 2017. pp. 101–9.
46. Dueñas-Mas MJ, Soriano ML, Ruiz-Palomero C, Valcárcel M. Modified nanocellulose as promising material for the extraction of gold nanoparticles. Microchem J. 2018;138:379–83.
47. Cieśla J, Chylińska M, Zdunek A, Szymańska-Chargot M. Effect of different conditions of synthesis on properties of silver nanoparticles stabilized by nanocellulose from Carrot pomace. Carbohydr Polym. 2020;245:116513.
48. Zhang K, Shen M, Liu H, Shang S, Wang D, Liimatainen H. Facile synthesis of palladium and gold nanoparticles by using dialdehyde nanocellulose as template and reducing agent. Carbohydr Polym. 2018;186:132–9.
49. Zhang X, Sun H, Tan S, Gao J, Fu Y, Liu Z. Hydrothermal synthesis of ag nanoparticles on the nanocellulose and their antibacterial study. Inorg Chem Commun. 2019;100:44–50.
50. Dufresne A. Nanocellulose: a new ageless bionanomaterial. Mater Today. 2013;16(6):220–7.
51. Xue Y, Mou Z, Xiao H. Nanocellulose as a sustainable biomass material: structure, properties, present status and future prospects in biomedical applications. Nanoscale. 2017;9(39):14758–81.
52. Norizan MN, Shazleen SS, Alias AH, Sabaruddin FA, Asyraf MRM, Zainudin ES, et al. Nanocellulose-based nanocomposites for sustainable applications: a review. Nanomaterials. 2022;12(19):3483.
53. Thomas B, Raj MC, Joy J, Moores A, Drisko GL, Sanchez C. Nanocellulose, a versatile green platform: from biosources to materials and their applications. Chem Rev. 2018;118(24):11575–625.
54. Li J, Hu J, Xiao L, Wang Y, Wang X. Interaction mechanisms between α-Fe_2O_3, γ-Fe_2O_3 and Fe_3O_4 nanoparticles and *Citrus maxima* seedlings. Sci Total Environ. 2018;625:677–85.
55. Mahmoud AWM, Ayad AA, Abdel-Aziz HS, Williams LL, El-Shazoly RM, Abdel-Wahab A, Abdeldaym EA. Foliar application of different iron sources improves morpho-physiological traits and nutritional quality of broad bean grown in sandy soil. Plants. 2022;11(19):2599.
56. Farooq A, Khan I, Shehzad J, Hasan M, Mustafa G. Proteomic insights to Decipher nanoparticle uptake, translocation, and intercellular mechanisms in plants. Environ Sci Pollut Res. 2024;31(12):18313–39.

57. Huong TT, Tuan TT, Duc HH, Ngoc PB, Ha CH, Nhut DT. Hardening of plantlets regenerated from Transgenic hairy roots of *Panax Vietnamensis* on medium containing iron nanoparticles. Metal nanoparticles in plant cell. Tissue and Organ Culture: Springer; 2024. pp. 249–75.
58. Ahmad A, Javad S, Iqbal S, Shahid T, Naz S, Shah AA, et al. Efficacy of soil drench and foliar application of iron nanoparticles on the growth and physiology of *Solanum lycopersicum* L. exposed to cadmium stress. Sci Rep. 2024;14(1):27920.
59. Rui M, Ma C, Hao Y, Guo J, Rui Y, Tang X, et al. Iron oxide nanoparticles as a potential iron fertilizer for peanut (*Arachis hypogaea*). Front Plant Sci. 2016;7:815.
60. Ortiz A, Sansinenea E. The role of beneficial microorganisms in soil quality and plant health. Sustainability. 2022;14(9):5358.
61. Malekzadeh E, Aliasgharzad N, Majidi J. Contribution of glomalin produced by rhizophagus irregularis to root stabilization of cd by white clover (*Trifolium repens* L). Appl Soil Res. 2016;4(1):1–13.
62. Velásquez A, Valenzuela M, Carvajal M, Fiaschi G, Avio L, Giovannetti M, et al. The arbuscular mycorrhizal fungus *Funneliformis Mosseae* induces changes and increases the concentration of volatile organic compounds in *Vitis vinifera* Cv. Sangiovese leaf tissue. Plant Physiol Biochem. 2020;155:437–43.
63. Güneş H, Demir S, Durak ED, Boyno G. The effect of arbuscular mycorrhizal fungal species *Funneliformis Mosseae* and Biochar against *Verticillium dahliae* in pepper plants under salt stress. Eur J Plant Pathol. 2024;170:669–86.
64. Bilgili A. The effectiveness of arbuscular mycorrhizal fungal species (*Funneliformis mosseae*, *Rhizophagus intraradices*, and *Claroideoglomus etunicatum*) in the biocontrol of root and crown rot pathogens, *Fusarium Solani* and fusarium mixture in pepper. PeerJ. 2025;13:e18438.
65. Řezáčová V, Némethová E, Stehlíková I, Czakó A, Gryndler M. Arbuscular mycorrhizal fungus *Funneliformis Mosseae* improves soybean growth even in soils with good nutrition. Microbiol Res. 2023;14(3):1252–63.
66. Singh M, Chauhan A, Srivastava DK, Singh PK. Arbuscular mycorrhizal fungi promote growth and enhance the accumulation of bioactive compounds in tomato (*Solanum lycopersicum* L). Biol Futura. 2024;75(2):251–7.
67. Singh M, Singh PK. Enhancing growth and drought tolerance in tomato through arbuscular mycorrhizal symbiosis. Rodriguésia. 2024;75:e00482024.
68. Andrino A, Guggenberger G, Kernchen S, Mikutta R, Sauheitl L, Boy J. Production of organic acids by arbuscular mycorrhizal fungi and their contribution in the mobilization of phosphorus bound to iron oxides. Front Plant Sci. 2021;12:661842.
69. Rajapitamahuni S, Kang BR, Lee TK. Exploring the roles of arbuscular mycorrhizal fungi in plant–iron homeostasis. Agriculture. 2023;13(10):1918.
70. Wahab A, Muhammad M, Munir A, Abdi G, Zaman W, Ayaz A, et al. Role of arbuscular mycorrhizal fungi in regulating growth, enhancing productivity, and potentially influencing ecosystems under abiotic and biotic stresses. Plants. 2023;12(17):3102.
71. Boyno G, Demir S, Rezaee Danesh Y, Durak ED, Çevik R, Farda B, et al. A new technique for the extraction of arbuscular mycorrhizae fungal spores from rhizosphere. J Fungi. 2023;9(8):845.
72. Senthilkumar M, Amaresan N, Sankaranarayanan A, Senthilkumar M, Amaresan N, Sankaranarayanan A. Isolation, enumeration of spores, and inoculum production of arbuscular mycorrhizal (AM) fungi. New York, NY: Springer Protocols Handbooks;: Humana; 2021.
73. Yousefi H, Faezipour M, Hedjazi S, Mousavi MM, Azusa Y, Heidari AH. Comparative study of paper and nanopaper properties prepared from bacterial cellulose nanofibers and fibers/ground cellulose nanofibers of Canola straw. Ind Crops Prod. 2013;43:732–7.
74. Yousefi H, Nishino T, Shakeri A, Faezipour M, Ebrahimi G, Kotera M. Water-repellent all-cellulose nanocomposite using silane coupling treatment. J Adhes Sci Technol. 2013;27(12):1324–34.
75. Koksal N, Agar A, Yasemın S. The effects of top coat substrates on seedling growth of marigold. J Appl Biol Sci. 2015;9(3):66–72.
76. Dhakal M, Pun AB, Bhattarai S. Effect of different planting time and varieties on growth and yield of African marigold (*Tagetes erecta*) in the Kavre district, Nepal. Nepal J Sci Technol. 2021;20(1):20–8.
77. Berimavandi AR, Hashemabadi D, Ghaziani MVF, Kaviani B. Effects of plant density and sowing date on the growth, flowering and quantity of essential oil of *Calendula officinalis* L. J Med Plants Res. 2011;5(20):5110–5.
78. Ahmad I, Jabeen N, Ziaf K, Dole J, Khan M, Bakhtavar M. Macronutrient application affects morphological, physiological, and seed yield attributes of *Calendula officinalis* L. Can J Plant Sci. 2017;97(5):906–16.
79. Dixit R, Rani M, Kumar J. Responses to different dosages of monocrotophos and deltamethrin on chlorophyll and protein contents of Chickpea. SAARC J Agric. 2023;21(1):217–25.
80. Sparks DL, Page AL, Helmke PA, Loeppert RH. Methods of soil analysis, part 3: chemical methods. Wiley; 2020.
81. Katyal J, Sharma B. A new technique of plant analysis to resolve iron chlorosis. Plant Soil. 1980;55:105–19.
82. Ahmed HF, Seleiman MF, Mohamed IA, Taha RS, Wasonga DO, Battaglia ML. Activity of essential oils and plant extracts as biofungicides for suppression of soil-borne fungi associated with root rot and wilt of marigold (*Calendula officinalis* L). Horticulturae. 2023;9(2):222.
83. Jaimand K, Bagher Rezaee M, Homami S. Comparison extraction methods of essential oils of *Rosmarinus officinalis* L. In Iran by microwave assisted water distillation; water distillation and steam distillation. J Med Plants By-Products. 2018;7(1):9–14.
84. Kumar A, Gautam RD, Kumar A, Bisht A, Singh S. Floral biology of wild marigold (*Tagetes Minuta* L.) and its relation to essential oil composition. Ind Crops Prod. 2020;145:111996.
85. Sun X-G, Tang M. Comparison of four routinely used methods for assessing root colonization by arbuscular mycorrhizal fungi. Botany. 2012;90(11):1073–83.
86. Cirtiu CM, Dunlop-Briere AF, Moores A. Cellulose nanocrystallites as an efficient support for nanoparticles of palladium: application for catalytic hydrogenation and heck coupling under mild conditions. Green Chem. 2011;13(2):288–91.
87. Eslami S, Ebrahimzadeh MA, Biparva P. Green synthesis of safe zero valent iron nanoparticles by *Myrtus communis* leaf extract as an effective agent for reducing excessive iron in iron-overloaded mice, a thalassemia model. RSC Adv. 2018;8(46):26144–55.
88. Kwon SS, Kong BJ, Cho WG, Park SN. Formation of stable hydrocarbon oil-in-water nanoemulsions by phase inversion composition method at elevated temperature. Korean J Chem Eng. 2015;32:540–6.
89. Shahrekizad M, Gholamalizadeh Ahangar A, Mir N. EDTA-coated Fe_3O_4 nanoparticles: a novel biocompatible fertilizer for improving agronomic traits of sunflower (*Helianthus annuus*). J Nanostruct. 2015;5:117–27.
90. Bhandari NS, Srivastava R, Tarakeshwari K, Chand S. Effect of nano and macro iron sprays on growth, flowering, seed and oil yielding attributes in calendula (*Calendula officinalis* L). J Hortic Sci. 2022;17(2):353–62.
91. Elfeky SA, Mohammed MA, Khater MS, Osman Y, Elsherbini E. Effect of magnetite nano-fertilizer on growth and yield of *Ocimum basilicum* L. Int J Indig Med Plants. 2013;46(3):1286–11293.
92. Khanizadeh P, Mumivand H, Morshedloo MR, Maggi F. Application of Fe_2O_3 nanoparticles improves the growth, antioxidant power, flavonoid content, and essential oil yield and composition of *Dracocephalum kotschyi* Boiss. Front Plant Sci. 2024;15:1475284.
93. Kreslavski V, Ivanov A, Shmarev A, Khudyakova A, Kosobryukhov A, editors. Influence of iron nanoparticles (Fe_3O_4 and Fe_2O_3) on the growth, photosynthesis and antioxidant balance of wheat plants (*Triticum aestivum*). BIO Web of Conferences; 2022: EDP Sciences.
94. Sun H, Qu G, Li S, Song K, Zhao D, Li X, et al. Iron nanoparticles induced the growth and physio-chemical changes in *Kobresia capillifolia* seedlings. Plant Physiol Biochem. 2023;194:15–28.
95. Zia-ur-Rehman M, Mfarrej MFB, Usman M, Anayatullah S, Rizwan M, Alharby HF, et al. Effect of iron nanoparticles and conventional sources of Fe on growth, physiology and nutrient accumulation in wheat plants grown on normal and salt-affected soils. J Hazard Mater. 2023;458:131861.
96. Zheng T, Zhou Q, Tao Z, Ouyang S. Magnetic iron-based nanoparticles biogeochemical behavior in soil-plant system: A critical review. Sci Total Environ. 2023;904:166643.
97. Tung HT, Phong TH, Nguyen PLH, Nghia LT, My HT, Ngan DMC, et al. Iron nanoparticles on growth and acclimatization of *Chrysanthemum morifolium* Ramat. Cv. Jimba in different culture systems. J Biotechnol. 2020;18(2):307–19.
98. Ngan HTM, Tung HT, Van Le B, Nhut DT. Evaluation of root growth, antioxidant enzyme activity and mineral absorbability of carnation (*Dianthus caryophyllus* express golem) plantlets cultured in two culture systems supplemented with iron nanoparticles. Sci Hort. 2020;272:109612.
99. Naseer M, Yang Y-M, Zhu Y, Zhao L, Cao J, Wang S, et al. Nano-iron and AM fungi inoculation in dryland wheat field: A sustainable alternative to plastic film mulching. Field Crops Res. 2024;306:109208.
100. Yang Y-M, Naseer M, Zhu Y, Wang B-Z, Zhu S-G, Chen Y-L, et al. Iron nanostructure primes arbuscular mycorrhizal fungi symbiosis tightly connecting maize leaf photosynthesis via a nanofilm effect. ACS Nano. 2024;18(31):20324–39.

101. Kanjana D. Foliar study on effect of iron oxide nanoparticles as an alternate source of iron fertilizer to cotton. Int J Chem Stud. 2019;7(3):4374–9.
102. Konate A, Wang Y, He X, Adeel M, Zhang P, Ma Y, et al. Comparative effects of nano and bulk-Fe_3O_4 on the growth of cucumber (*Cucumis sativus*). Ecotoxicol Environ Saf. 2018;165:547–54.
103. Yuan J, Chen Y, Li H, Lu J, Zhao H, Liu M, et al. New insights into the cellular responses to iron nanoparticles in *Capsicum annuum*. Sci Rep. 2018;8(1):1–9.
104. Li M, Zhang P, Adeel M, Guo Z, Chetwynd AJ, Ma C, et al. Physiological impacts of zero valent iron, Fe_3O_4 and Fe_2O_3 nanoparticles in rice plants and their potential as Fe fertilizers. Environ Pollut. 2021;269:116134.

Publisher's note